

# NUMERICAL STUDY ON THE RECOATING PROCESS IN MICROSTEREOLITHOGRAPHY

W. Tan, and I. Gibson

Department of Mechanical Engineering, the University of Hong Kong, Hong Kong

Reviewed, accepted August 3, 2005

## Abstract

Microstereolithography is a promising RP-based micro-fabrication technique that aims to meet the demands for complex geometry micro-scale parts. Projection microstereolithography incorporates a Dynamic Pattern Generator to obtain high resolution in the parallel plane. However, its lateral resolution has been always limited by the final layer thickness and the long resin settling time, both of which rely on the recoating process. In order to find the critical factors behind the recoating process, a numerical simulation method (Computational Fluid Dynamics, CFD) has been used to investigate the relationships among final layer thickness, settling time, resin viscosity and ratio of object/container size. These results are helpful for the selection of resin characteristics and the design of the microstereolithography machine.

**Keywords:** microstereolithography, recoating process, numerical simulation

## 1. Introduction

Product miniaturization is an emerging technology trend in today's industry, which demands a large amount of smaller parts and components, such as micromechanical components for medical devices, miniature electrical connector, micro fluid device and chemical reactors, etc. The study report from influential European Network of Excellence in Multifunctional Microsystems (NEXUS) predicts the microsystem market potential will increase from about \$40 billion in 2002 to \$68 billion by 2005 [1].

Today, a variety of microfabrication techniques have been developed to meet this demand. Conventional microfabrication methods such as silicon-based micromachining and LIGA (based on lithography, electroforming, and moulding) allow the manufacturing of many different microstructures and components [2]. However, most of these components are still quasi two-dimensional; their geometry is quite simple and the manufacture lacks flexibility. For these conventional microfabrication techniques, it is far from the solid freeform microfabrication that we are familiar with.

Microstereolithography, which came forth in 1993 for the first time, is a new 3D freeform microfabrication process that is derived from the stereolithography technique currently used in the conventional rapid prototyping industry [3]. Several research groups around the world have developed different microstereolithography processes, such as the IH process, 2-photon process, integral process, etc [3][4][5]. In order to obtain higher resolution than conventional stereolithography, they adopted different improvements in the basic design (for example, better focusing to reduce laser spot size and controlling the penetration depth). In general, comparing to

the resolution of 50-200  $\mu\text{m}$  in conventional stereolithography, microstereolithography has obtained a resolution as high as several microns and even submicron. This significant improvement in resolution enables microstereolithography to build small 3D components with high-aspect ratio.

Another important advantage is that microstereolithography allows the fabrication of almost any geometry, whatever its complexity. This feature of freeform fabrication benefits from the working principle inherited from stereolithography. That is, a 3D model is sliced into a succession of thin layers following the CAD process, and each layer can be regarded as a 2D pattern, which is used to control the light source to solidify a layer of liquid resin selectively. In this manner, combining layer upon layer, a complex solid object is built.

## **2. Microstereolithography and Recoating Process**

### **2.1 Microstereolithography**

Although all are based on light-induced polymerization, in terms of fabrication method used, the various microstereolithography processes can generally be classified into two main categories: scanning method and projection method [6]. Each has its own advantages and disadvantages and is suitable for different applications.

#### **Scanning method**

In scanning methods, each layer is built with a point light source in a line-by-line way, which is the same as conventional stereolithography. Microstereolithography systems adopting scanning method include the IH process, super IH process and two-photon process et al.

The IH (Integrated Harden polymer stereolithography) process was the first microstereolithography technique, presented by Ikuta and Katagi in 1993 [5][7]. Figure 1 shows its system diagram. In the IH process, UV light was focused onto the resin surface through a glass window, which led to two benefits. The first benefit is that the focus point was fixed during fabrication, which produces a smaller focus spot and higher lateral resolution. The second benefit is that a glass window was attached to the Z-stage for precise layer-thickness preparation, consequently improving the resolution in depth. The minimum size of hardened polymer unit is  $5\ \mu\text{m} \times 5\ \mu\text{m} \times 5\ \mu\text{m}$ .

Based on the IH process, Ikuta proposed a Mass-IH process in 1996 [8]. An array of single-mode optical fibres was used to fabricate multiple objects simultaneously. In 1998, he presented the super IH process [9]. The laser beam was focused into liquid resin and solidification took place inside the medium instead of on the surface. Hence, no layer preparation was required and the resolution improved to submicron level.

Maruo et al. presented another type of scanning microstereolithography process based on two-photon absorption [4]. Its system is similar to super IH process. Since two-photon based

polymerization happens only in a small volume within the focal depth, it reduces greatly the unwanted polymerization taking place in other types of microstereolithography and increases the accuracy of fabrication. However, two-photon process is much more expensive than others.

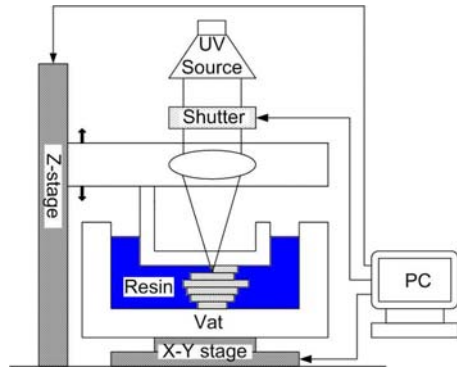


Fig.1 IH System (from [5])

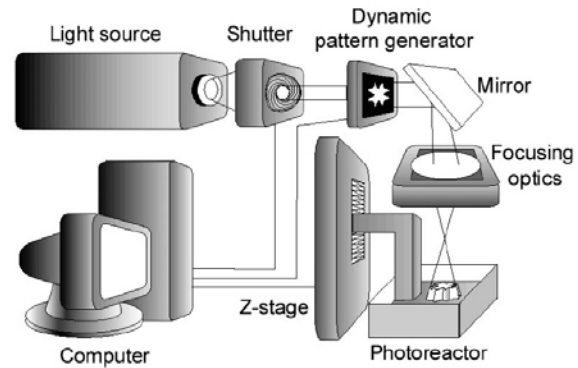


Fig.2 Projection System (from [3])

### Projection process

Comparing with the manner of line-by-line fabrication, this technique allows each layer to be built with a single exposure, consequently improving the fabrication accuracy to a certain extent. A 3D model is sliced in a computer, generating a succession of 2D slices. Each slice is converted to a bitmap file, which is used to drive the dynamic pattern generator. The beam coming from light source is modulated by the pattern generator to contain the shape of the layer to be built. Then, the light beam shape is focused on the liquid resin's surface through optical components, solidifying one layer selectively with the expected shape. After one layer is finished, the object being built is recoated by a second layer of fresh resin. Then, solidification of the next layer begins. These steps repeat until the whole object is fabricated.

Dynamic pattern generator is the critical component in the projection process. Two kinds of devices can provide this role: liquid crystal display (LCD) and digital micromirror device (DMD). Both can be used to form an array of pixels. Each pixel can switch the light transmission on or off, consequently modulating the light passing through it. The first projection microstereolithography using LCD was proposed by Bertsch in 1995 [3]. Loubère et al. developed another projection system using LCD as pattern generator, which utilized halogen lamp instead of laser as the light source in 1998 [10]. At the same year, Chatwin et al. presented a UV projection microstereolithography system [11].

The major advantage of projection microstereolithography is in terms of the speed. Since the layer thickness must be very thin, the light intensity must be kept low and therefore the reaction times are subsequently much longer than conventional stereolithography. By projecting in a single step, an entire layer can be polymerised thus reducing the time per layer. The objective of the research related to this paper is to focus on further reducing the time per layer by examining the way the resin behaves in the process.

## 2.2 Recoating Process

For microstereolithography processes which fabricate objects inside the medium (for example, the super IH and two-photon processes), no recoating process is required. However, for those fabricating on the surface (projection process et al), the recoating process is crucial for the resolution in the depth dimension. Layer thickness for conventional stereolithography is 50-200 $\mu\text{m}$ . Its precision is guaranteed through use of a scraper or blade. In microstereolithography, layer thickness is less than 10 microns, in which no scraper can be used for fear of deformation and destruction of objects being built. For research consideration, the recoating process mentioned below refers to that of the projection process.

The basic operation for recoating a new resin layer is illustrated in Figure 3. After one layer is polymerized (Figure 4(a)), the Z-stage moves downwards, and the object is immersed deeply into the resin vat, ensuring the surface of the already solidified layer is fully covered by liquid resin (Figure 4(b)). Then, the Z-stage moves upwards and lifts up the object close to resin's surface (Figure 4(c)). At the moment when the part reaches this position, the resin close to the new layer is still in motion. The system must wait for the resin surface to settle under gravity before fabrication can resume. This kind of recoating process is also called the "deep-dip" process.

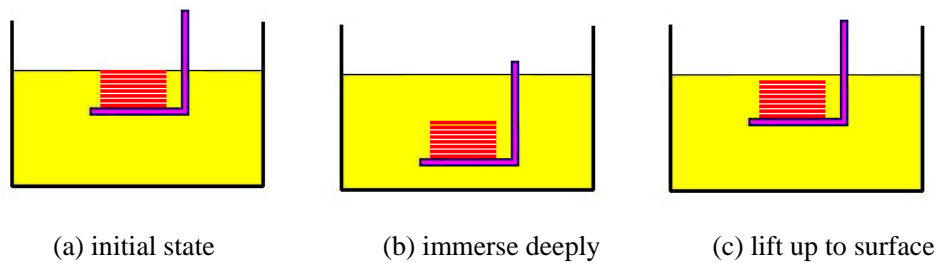


Fig.3 Recoating process in projection microstereolithography

The operation of layer preparation seems very simple. However, it is hard to obtain a uniform fresh layer with a thickness of only several microns in realistic operation. In microstereolithography, this recoating process leads to limitations in minimum layer thickness because of the resin's viscosity and surface tension. Furthermore, it has to spend a large amount of time waiting for the resin to settle under gravity, unavoidably decreasing the building speed. Typically, for each layer, it is 1 second for the fabrication, but it is at least 10-15 seconds for resin's recoating (and can be as long as 1 minute or more) [12].

For the reasons mentioned above, the recoating process has direct impact on the resolution in depth dimension and also significantly affects the build time. It is one of the most important and interesting problems worth investigated in projection microstereolithography. Currently there are no quantitative criteria that exist to tell whether and when the surface of fresh resin is horizontal and stable enough to proceed. Also few researchers have studied the effect of the resin's rheological properties on the settling time. Here, the authors have attempted to simulate the

recoating process numerically.

### 3. Numerical Simulation Method

#### 3.1 CFD fundamentals

In the recoating process, resin motion is treated as laminar flows of various incompressible fluids. Although the final thickness of each fresh layer may be only a few microns, this still belongs to macroscopic length scales, and molecular effects may be ignored. Hence, the resin movement conforms to Navier-Stokes equations. For the two-dimensional case, its governing equations are as follows [13]:

*Momentum equations:*

$$\rho \frac{Du}{Dt} = \frac{\partial(-p + \tau_{xx})}{\partial x} + \frac{\partial \tau_{yx}}{\partial y} + S_{Mx} \quad (1)$$

$$\rho \frac{Dv}{Dt} = \frac{\partial \tau_{xy}}{\partial x} + \frac{\partial(-p + \tau_{yy})}{\partial y} + S_{My} \quad (2)$$

*Continuity equation:*

$$\frac{\partial u}{\partial x} + \frac{\partial v}{\partial y} = 0 \quad (3)$$

Here,  $u$  and  $v$  are the velocity vectors in  $x$  and  $y$  directions respectively,  $p$  is pressure,  $\tau_{xy}$ ,  $\tau_{yx}$ ,  $\tau_{xx}$  and  $\tau_{yy}$  stand for stress components,  $S_{Mx}$  and  $S_{My}$  denote body forces only, such as gravity. The effects of surface forces are accounted for explicitly (i.e. a surface stress is the product of stress and area) in equations (1) and (2).

In order to solve the partial differential equations (1), (2) and (3) numerically, the fluid flow problems have to be represented in a discrete manner. That is to say, the fluid continuum is replaced by a mesh of discrete points, which is the same as for the time variable. Thus, using different discretization methods, the problem involving calculus can be transformed into an algebraic problem.

#### 3.2 Method description

Resin motion in the recoating process is modelled as a free surface flow driven by submerged objects. Resin viscosity and surface tension are both taken into consideration. The quantity under consideration is the shape of the resin's surface in terms of time, through which the settling time can be determined [14].

FLUENT is a leading CFD software package for general fluid simulation, which contains various fluid dynamics models and is able to solve many different problems. Among them, the

Volume of Fraction (VOF) model is chosen to simulate this free surface flow. VOF model is a multiphase model, which uses  $\alpha_q$  to indicate the volume fraction of phase  $q$  in each computation cell. It also includes viscosity and surface tension into computation. This is very suitable for transient (time-dependent, that is unsteady) tracking of the fluctuation at the interface of liquid and air [15]. In addition, a User Defined Function (UDF) program has been written to define the motion of the object and the reconstruction of dynamic mesh zone.

Figure 4 shows the transient shape of resin's surface when an object stops the upward motion. The extracted data of surface shape is shown in Figure 5 using different scaling for each axis. The dash line is the initial surface level before deep-dip process. From Figure 5, the average thickness of fresh resin stacked on the solidified object is about 200  $\mu\text{m}$ . Using this method to calculate more time steps, the simulation will find when the thickness decreases to less than 10  $\mu\text{m}$ .

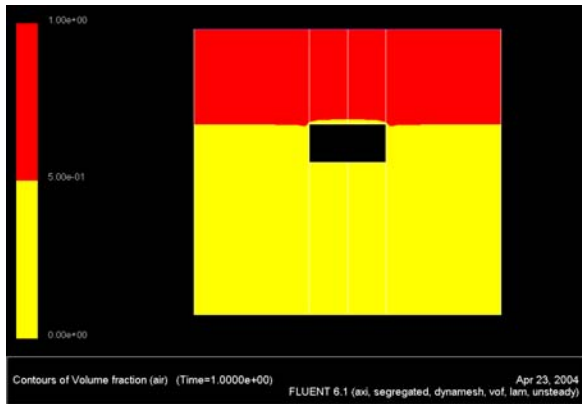


Fig.4 Surface profile after translation

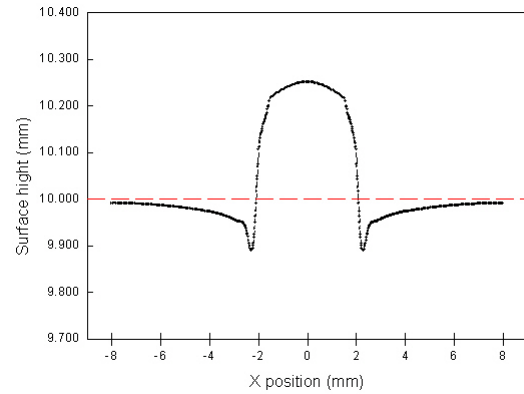


Fig.5 Surface curve extracted

#### 4. Results and Discussions

Using the method described above, simulations have been carried out mainly to investigate resin viscosity effects and object/vat size ratio effects during recoating process. The initial condition for each simulation was set so that no motion existed in the whole computational domain, and the shapes of the object and resin vat were both cylindrical (i.e. axi-symmetrical). Then, the object's translation motion was applied. In order to investigate resin viscosity effects, four viscosities (0.1, 0.3, 1 and 3cp) and two different object sizes (1.6mm and 3.2mm in radius) have been investigated. The resin vat dimension was fixed (49.6mm in radius) and the translation scheme was fixed for all cases. For investigation of size effects, four different object sizes (0.8mm, 1.6mm, 3.2mm and 6.4mm in radius) were then selected to obtain different object/vat size ratios. Since the resin's motion during the translation period was not our concern, settling time in all results started from the time when the translation motion stops. The results are listed below.

##### 4.1 Viscosity effect

Figure 6 shows the average layer thickness-time curves under four different viscosities, when the object radius is 1.6mm. Figure 7 shows the same results, but the object radius is 3.2mm. All the curves indicate that the average thickness decreases quickly at the beginning of the settling period, and then reaches to a stable thickness gradually and continuously. This stable layer thickness can be regarded as the final layer thickness that can be achieved under that case. At the same time, the settling time required for the stable state can be estimated from these curves.

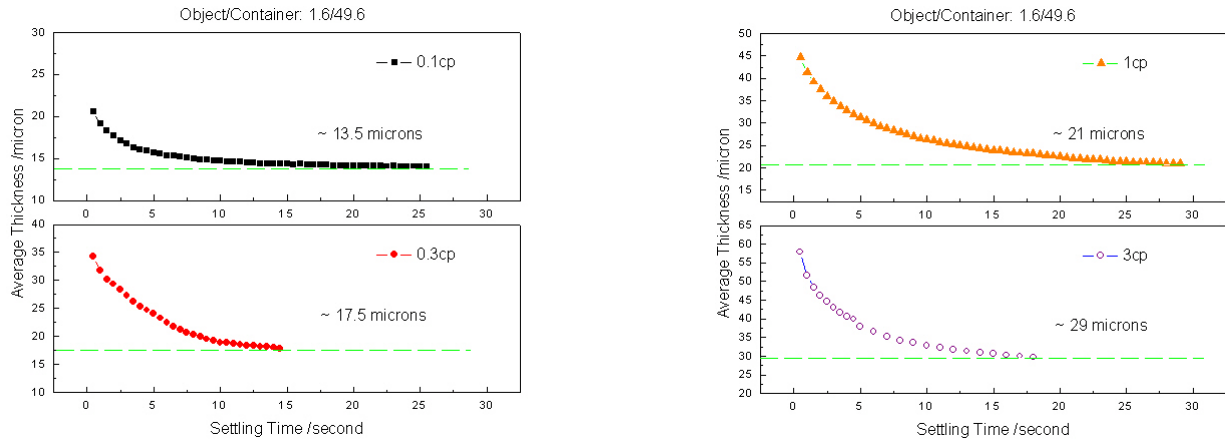


Fig.6 Average Thickness under different time  
(Viscosity: 0.1, 0.3, 1 and 3cp, object radius: 1.6)

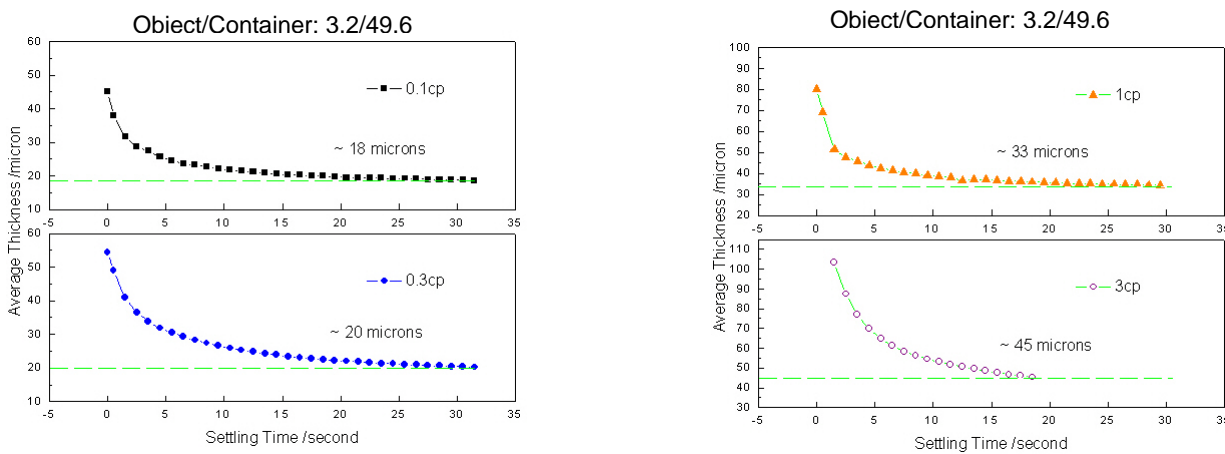


Fig.7 Average Thickness under different time  
(Viscosity: 0.1, 0.3, 1 and 3cp, object radius: 3.2)

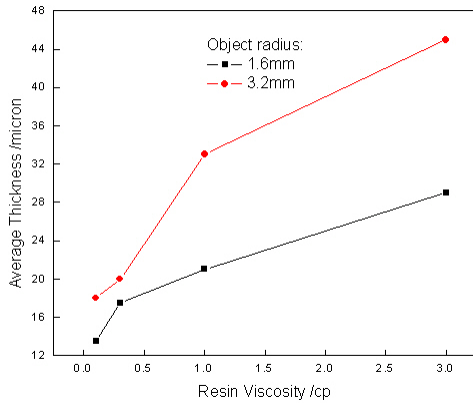
### Viscosity effects on final thickness

From Figure 6, the final layer thicknesses are 13.5 $\mu$ m for 0.1cp, 17.5 $\mu$ m for 0.3cp, 21 $\mu$ m for 1cp and 29 $\mu$ m for 3cp respectively when the object radius is 1.6mm. From Figure 7, the final layer thicknesses are 18 $\mu$ m for 0.1cp, 20 $\mu$ m for 0.3cp, 33 $\mu$ m for 1cp and 45 $\mu$ m for 3cp respectively when the object radius is 3.2mm. Figure 8 summarizes the final thickness' variation with viscosity. It indicates that 1) viscosity is a critical factor for the final layer thickness, and smaller layer thickness can be obtained with lower viscosity under gravity leveling; 2) in order to

obtain a layer thickness less than 10 $\mu$ m in projection microstereolithography, resin viscosity expected should be close to or below 0.1cp; 3) some methods should be carried out to decrease current resins' higher viscosities before adopting them in projection microstereolithography.

### Viscosity effects on settling time

Table 1 summary the settling time under four viscosities. It shows that lower viscosity may be helpful for resin's settling, however lower viscosity doesn't ensure shorter settling time.



Viscosity/cp	3	1	0.3	0.1
Settling time 1.6/49.6	-	25s	15s	16s
Settling time 3.2/49.6	-	22s	27s	25s

Fig. 8 Final Thickness under different viscosity      Tab. 1 Settling time under different viscosity

### 4.2 Size ratio effect

Figure 9 shows the average layer thickness-time curves under different object size (i.e. different object/vat size ratio, since vat size was fixed). All parameters and conditions are the same except the object size. All the curves share the same variation tendency, the average thickness decreasing quickly at the beginning of the settling period, and then reaching to a stable thickness gradually and continuously. However, the final layer thickness reached and settling time is different.

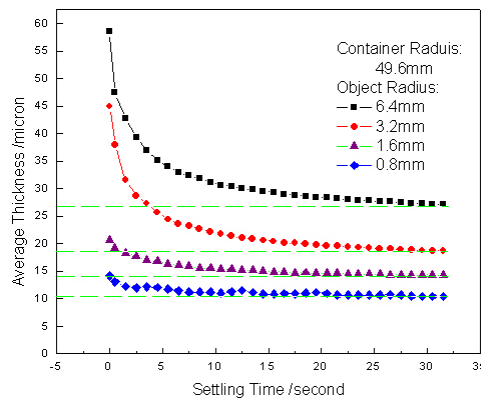


Fig. 9 Average thickness under different time  
(Viscosity: 0.1cp, object radius: 0.8, 1.6, 3.2 and 6.4mm)

### Size ratio effect on final thickness

From figure 9, the final layer thicknesses are  $10.5\mu\text{m}$  for  $0.8\text{mm}$ ,  $13.5\mu\text{m}$  for  $1.6\text{mm}$ ,  $18\mu\text{m}$  for  $3.2\text{mm}$  and  $27\mu\text{m}$  for  $6.4\text{mm}$  respectively. Figure 10 summaries final layer thickness' variation under different object/vat size ratio. It shows that 1) object/vat size ratio is a critical factor for the final layer thickness; 2) smaller final thickness can be achieved when adopting smaller the object/vat size ratio; 3) in order to obtain layer thickness close to or below  $10\mu\text{m}$  in projection microstereolithography, the ratio expected should be close to or below  $0.02$ ; 4) large resin vat is recommended for smaller layer thickness.

### Size ratio effect on settling time

Figure 11 summarizes the settling time required for stable state under different object/vat size ratio. It shows that 1) settling time decreases as the ratio of object/vat size decreases; 2) object/vat size ratio affects the settling time significantly and consistently; 3) larger resin vat is helpful for shortening the settling time.

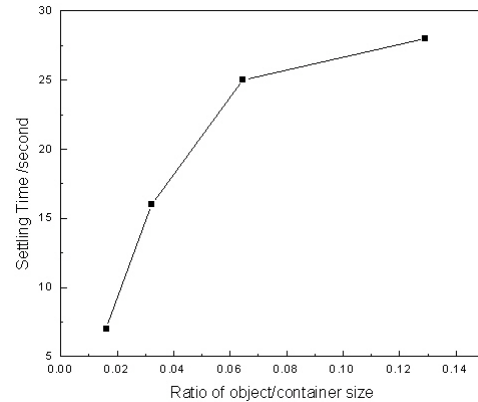
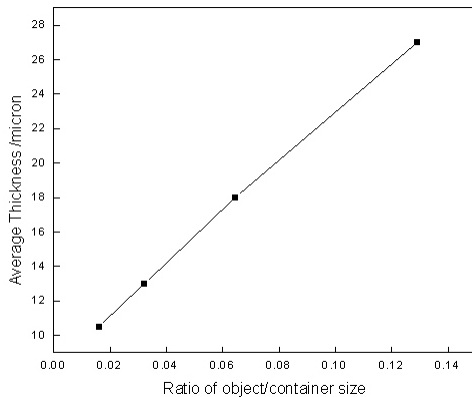


Fig.10 Final thickness under different size ratio

Fig.11 Settling time under different size ratio

This paper mainly presents the simulation results on the effect of resin viscosity and object/vat size ratio. There are still some other factors that play important roles in the recoating process, such as temperature differential in the resin vat and object's asymmetry in practical fabrication. These factors will be investigated in later work.

## 5. Conclusions

Recoating process determines the depth resolution in projection microstereolithography. However, it is hard to evaluate the critical working parameters in the recoating process. This paper has presented a numerical simulation method to investigate the recoating process. The results indicate that both resin viscosity and object/vat size ratio play important roles in the recoating process. Low viscosity resins and small object/vat size ratio are recommended.

At the same time, there is still future work that needs to be done, that is to obtain experimental results to compare with the simulation result. It is hoped that this method can find

some ways to improve the accuracy of layer thickness and accelerate build time, and the results are helpful for the selection of resin characteristics and the design of further microstereolithography machines.

### References

- 1 <http://www.sgt-sensor.de/NEXUS.html>
- 2 **Bang C., Melzak J., and Mehregany M.,** (1994) From Microchips to MEMS, Microlithography World Spring. pp. 15-16.
- 3 **Bertsch A., Bernhard P., et al.,** (2001) Microstereolithography: Concepts and applications. Etfa 2001: 8th Ieee International Conference on Emerging Technologies and Factory Automation, Vol 2, Proceedings. New York, IEEE, pp. 289-298.
- 4 **Maruo S., and Kawata S.,** (1998) Two-photon-absorbed near-infrared photo-polymerization for three-dimensional microfabrication. J. Microelectromech. Syst., 7(4), pp. 411-415.
- 5 **Ikuta K., and Hirowatari K.,** (1993) Real three dimensional microfabrication using stereo lithography and metal modelling. Proc. IEEE MEMS, pp. 42-47.
- 6 **Varadan V. K., Jiang X., and Varadan V. V.,** (2001) *Microstereolithography and other Fabrication Techniques for 3D MEMS*. John Wiley & Sons.
- 7 **Katagi T., and Nakagima N.,** (1993) Photoforming applied to fine machining. Proc. IEEE MEMS, pp. 173-178.
- 8 **Ikuta K., et al.,** (1996) Development of mass productive microstereolithography (Mass-IH process). Proc. MEMS, pp. 301-305.
- 9 **Ikuta K., Maruo S., and Kojima S.,** (1998) New microstereolithography for freely moved 3D micro structure – super IH process with submicron resolution. Proc. IEEE MEMS, pp. 290-295.
- 10 **Loubère V., Monneret S., and Corbel S.,** (1998) Microstereolithography using a mask-generator display. Proc. of the 4th Japan-France Congress and 2nd Asia-Europe Congress on Mechatronics, pp. 160-163.
- 11 **Chatwin C. R., Farsari M., et al.,** (1998) UV microstereolithography system that uses spatial light modulator technology. Applied Optics, vol. 37, pp. 7514-7522.
- 12 **Bertsch A., et al.,** (2000) Rapid prototyping of small size objects. Rapid Prototyping Journal 6 (4), pp. 259-266.
- 13 **Versteeg H. K., and Malalasekera W.,** (1995) *An Introduction to Computational Fluid Dynamics: the Finite Volume Method*. Prentice Hall.
- 14 **Tan W., and Gibson I.,** (2004) Microstereolithography and application of numerical simulation on its layer preparation. International Conference on Manufacturing Automation, pp. 675-682
- 15 *FLUENT 6.1 Help Documentation*. Fluent Inc.

### Acknowledgements

The research reported in the paper was supported by the studentship from Department of Mechanical Engineering at the University of Hong Kong.